



Cite this: *CrystEngComm*, 2026, 28, 1019

## Dimethylated $\beta$ -cyclodextrin inclusion complexes containing the guest steroid hormones progesterone and 17 $\beta$ -estradiol: syntheses, crystal structures, thermal analyses and steroid solubility enhancements

Alexios I. Vicatos, Zakiena Hoossen, Cesarina Edmonds-Smith and Mino R. Caira \*

Considerable ongoing research is aimed at enhancing the delivery of poorly soluble active pharmaceutical ingredients (APIs) *via* their complex formation with water-soluble cyclodextrin host compounds. The aim of the present study was to complex the potent steroidal hormones progesterone (PRO) and 17 $\beta$ -estradiol (BES) with heptakis(2,6-di-*O*-methyl)- $\beta$ -cyclodextrin (DMB), and to characterize the resulting complexes for assessment of their potential utility. Complex synthesis using co-precipitation methods yielded single crystals of the desired complexes, which were subsequently characterized by thermal analysis, single-crystal X-ray analyses and solubility measurements. <sup>1</sup>H NMR spectroscopy indicated 1:1 host-guest stoichiometries for both of the hydrated complexes DMB-PRO and DMB-BES. Thermal analysis showed that the dehydrated DMB-PRO complex remained intact up to a temperature of  $\sim$ 180  $^{\circ}$ C, when complex decomposition commenced. However, following the dehydration of DMB-BES, loss of the guest BES occurred in the approximate range 180–325  $^{\circ}$ C. Major findings were evident from X-ray analyses, which revealed only a single mode of API inclusion in the DMB-PRO crystal, but instead, the relatively rare phenomenon of bimodal API inclusion within the crystal of DMB-BES. Measurements of complex dissolution in a biorelevant medium at 27  $^{\circ}$ C showed significant API solubility enhancements of  $\sim$ 25-fold for PRO and  $\sim$ 40-fold for BES as a result of their inclusion in DMB.

Received 21st November 2025,  
Accepted 12th January 2026

DOI: 10.1039/d5ce01106j

[rsc.li/crystengcomm](http://rsc.li/crystengcomm)

### 1. Introduction

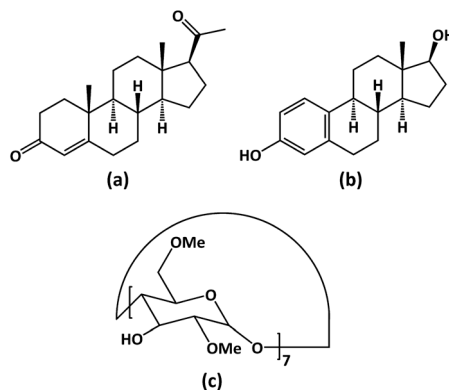
The use of cyclodextrins (CDs), macrocyclic oligosaccharides composed of  $\alpha$ -1,4-linked glucose molecules, or chemically modified glucose units, is a well-established technology for achieving solubilisation and more efficient delivery of poorly soluble molecules, including active pharmaceutical ingredients (APIs). Of the numerous reviews and monographs describing the structures, properties and the variety of applications of CDs, including drug delivery, several comprehensive reviews published in the last three years are cited here.<sup>1–4</sup> As illustrated in these reviews, the essential structural features of a CD that render it useful in this context are a central apolar cavity which can host a lipophilic API molecule *via* non-covalent interactions, and a hydrophilic exterior that enables dissolution of the resulting inclusion complex in aqueous media. Following *in vivo* administration of the formulated CD–drug complex, the

apparent solubility of the guest API molecules is thus increased and the enhanced rate of complex dissociation leads to elevated API concentration at biological membranes, and hence an increase in API bioavailability. Among the plethora of APIs and other bioactive compounds that have been investigated for potential inclusion complex formation with CDs, steroidal hormones that perform multiple functions in the human physiology of growth and development, energy metabolism, homeostasis and sexual reproduction, are very significant targets.<sup>5–7</sup> However, these steroids generally display poor aqueous solubility, which limits their bioavailability. In this report, the focus is on two steroids, progesterone (PRO, Scheme 1(a)) and 17 $\beta$ -estradiol (BES, Scheme 1(b)), both of which are prominent members of the class of female sex steroids, with complementary roles in menopausal therapy.<sup>8–10</sup>

We recently reported inclusion complexation of both PRO and BES molecules with the native cyclodextrins  $\beta$ -CD and  $\gamma$ -CD, and characterized the resulting crystalline complexes using thermal analysis techniques, <sup>1</sup>H NMR spectroscopy, and both powder and single-crystal X-ray diffraction (SCXRD).<sup>11</sup> With MoK $\alpha$  X-rays, the latter technique revealed that the PRO and BES molecules are severely disordered

Centre for Supramolecular Chemistry Research, Department of Chemistry,  
University of Cape Town, Rondebosch 7701, South Africa.  
E-mail: [mino.caira@uct.ac.za](mailto:mino.caira@uct.ac.za)





**Scheme 1** The chemical structures of progesterone (a), 17 $\beta$ -estradiol (b) and DMB (c).

within the cavities of these host molecules at 100 K and could not be modelled (more recently, however, a re-determination of the structure of the  $\beta$ -CD-BES complex at 100 K using CuK $\alpha$  X-rays enabled resolution of the disorder in the form of two BES components with equal site-occupancy within the  $\beta$ -CD cavity.)<sup>12</sup> In our previous study with  $\beta$ -CD and  $\gamma$ -CD as host molecules,<sup>11</sup> solubility measurements were also performed to assess the extent to which complexation between these native CDs and the APIs PRO and BES might have influenced the aqueous solubilities of the steroids. The results indicated modest solubility enhancement factors for PRO and BES of 20-fold and 5-fold respectively.

The limitations of our previous study with PRO and BES outlined above therefore prompted the present investigation, which focused on the isolation of inclusion complexes between PRO and BES with a well-known derivative of  $\beta$ -CD, namely heptakis(2,6-di-*O*-methyl)- $\beta$ -CD (aka dimethylated  $\beta$ -CD, or DMB) [Scheme 1(c)], given that its solubilizing power is approximately 30 times that of  $\beta$ -CD.<sup>13</sup> As reported in detail below, the target complexes were duly synthesized by the co-precipitation method and characterized using <sup>1</sup>H NMR spectroscopy to determine their host-guest stoichiometries. In addition, since the detailed modes of inclusion of steroid molecules encapsulated in hydrophobic CD cavities (*i.e.*, the relative orientations of host and guest molecules, and the depth of cavity penetration) affect both the steroidal API stability and the mechanism of their guest release,<sup>6,14</sup> X-ray structural analyses of the complexes were undertaken to establish the detailed host-guest inclusion modes. These goals were duly achieved and the results contribute to the relatively small knowledge base of the structural features of crystalline CD-steroid inclusion complexes, consisting of 11 entries in the Cambridge Structural Database,<sup>15</sup> of which 5 were reported from our laboratory. In particular, a remarkable structural feature of the DMB-BES complex determined in the present study is the occurrence of the rare phenomenon of bimodal guest inclusion,<sup>14,16,17</sup> manifested, in this instance, within the same crystal. Thermal analyses were employed to determine the solid-state stability of the inclusion complexes. Finally, the solubilities of PRO and BES resulting from their complexation

with DMB were measured in a more relevant medium than pure water, namely a simulated biological medium, these experiments yielding significant solubility enhancement factors of  $\sim$ 25-fold for PRO and  $\sim$ 40-fold for BES.

The recent, authoritative review by Fenyvesi *et al.*<sup>6</sup> focuses on steroidal drugs and their complexation with CDs, as well as aspects of major importance such as steroidal drug solubility, stability and bioavailability, and applications of encapsulated steroids. Given the context of the above review, the present study is more than justified, as it presents new findings on the complexation of the potent, but poorly water-soluble steroids PRO and BES, with the derivatised cyclodextrin DMB. This study included crystallization of the resulting inclusion complexes, their analysis by thermal methods to determine their stability, single crystal X-ray structures, and assessment of drug solubility enhancements achieved *via* their inclusion in DMB. Major novel features of the study include: (a) isolation and characterization of well-resolved complex structures *via* the use of DMB as host, lacking the extensive guest disorder previously observed with  $\beta$ -CD and  $\gamma$ -CD as hosts,<sup>11</sup> (b) the adoption of two distinct anisotropic BES inclusion modes within the same crystal, which has not been previously reported to the best of our knowledge, (c) contrasting shallow and deep guest molecule inclusion in DMB-BES, and (d) evidence of ‘mutual induced fit’ of host and guest molecules upon formation of both DMB-PRO and DMB-BES.

## 2. Experimental

### 2.1 Materials

The steroidal APIs progesterone (PRO, C<sub>21</sub>H<sub>30</sub>O<sub>2</sub>, purity > 98%) and 17 $\beta$ -estradiol (BES, C<sub>18</sub>H<sub>24</sub>O<sub>2</sub>, purity > 98%) were purchased from Sigma-Aldrich Chemie GmbH (Steinheim, Germany) and were used as received. Dimethylated  $\beta$ -CD [heptakis(2,6-di-*O*-methyl)- $\beta$ -cyclodextrin (DMB, C<sub>56</sub>H<sub>96</sub>O<sub>35</sub>)] with purity  $\sim$ 95% was acquired from Cyclolab R&D Ltd. (Budapest, Hungary). Milli-Q Water® (Millipore corporation, Billerica, Massachusetts, USA) was used as the medium for co-precipitation experiments. Fasted state simulated intestinal fluid (FaSSIF) was purchased from <http://Biorelevant.com> Ltd. (London, UK).

### 2.2 Complex synthesis by the co-precipitation method

The procedures for crystallizing the DMB complexes were based on the known negative solubility coefficients of methylated CDs, manifested in their ready dissolution in cold water and their crystallization at high temperature,<sup>18</sup> the latter behaviour also extending to complexes of DMB. To a vial containing a solution of DMB (48.9 mg, 0.0368 mmol) in 2.0 cm<sup>3</sup> Milli-Q water at 23 °C, BES (5.0 mg, 0.0184 mmol) was slowly added in small successive increments, with continuous stirring over a period of 2 h. In addition, temperature cycling was employed to effect more rapid dissolution of BES. Finally, the suspension was stirred for 24 h in a cold room maintained at 4 °C, during which complete dissolution took place. After filtering the cold



solution (0.45  $\mu\text{m}$  microfilter) into a clean pre-cooled vial, the latter was placed in an oven at 60  $^{\circ}\text{C}$ , to effect crystallization of the DMB-BES complex, which occurred after 3 days. A slightly modified procedure was necessary to isolate the DMB-PRO complex. An excess amount of DMB (42.34 mg, 0.0318 mmol) was dissolved in cold water. PRO (5.0 mg, 0.0158 mmol) was added incrementally with vigorous stirring but without temperature cycling. Complete dissolution of PRO occurred after stirring the solution in the cold room at 4  $^{\circ}\text{C}$  overnight. Complex crystallization was effected within 3 days by maintaining the vial at 60  $^{\circ}\text{C}$  in an oven while allowing excess water to evaporate gradually.

### 2.3 Stoichiometry determination using $^1\text{H}$ NMR spectroscopy

Accurately weighed samples of single crystals of each of the complexes DMB-PRO and DMB-BES with masses in the range 3–5 mg were dissolved in deuterated dimethyl sulfoxide (DMSO- $d_6$ ) and their  $^1\text{H}$  NMR spectra were recorded at 23  $^{\circ}\text{C}$  on a Bruker Ultrashield 400 Plus spectrometer (Billerica, MA, USA). The data were analysed using the program MestReNova.<sup>19</sup>

### 2.4 Complex characterization using thermal analysis

Micrographs of the behaviour of complex crystals during heating were captured using hot stage microscopy (HSM). Crystals were immersed in silicone oil and heated at 10  $\text{K min}^{-1}$  over the temperature range  $\sim 20$ –300  $^{\circ}\text{C}$  using a Linkam THMS600 apparatus attached to a TP92 temperature control unit (Linkam Scientific Instruments, Tadworth, UK). Significant thermal events were recorded on a Sony Digital Hyper HAD video camera (Sony Corporation, Tokyo, Japan) and were processed using the Soft Imaging System program analySIS.<sup>20</sup> The behaviour on heating the crystalline complexes was also examined using a TA-Q500 thermogravimetric analyser (TA Instruments, New Castle, DE, USA) at a heating rate of 10  $\text{K min}^{-1}$  with a dry  $\text{N}_2$  purge rate of 60  $\text{cm}^3 \text{min}^{-1}$ . Universal Analyzer software (v4.5A, TA Instruments-Waters LLC, New Castle, DE, United States) was used for data-processing. In addition, thermal events were recorded by differential scanning calorimetry (DSC) on a TA Discovery DSC 25 instrument (New Castle, DE, USA), with TRIOS software for data-processing.<sup>21</sup>

### 2.5 Structural analyses by single-crystal X-ray diffraction (SCXRD)

Intensity data for both hydrated complexes were collected using a Bruker Kappa Apex II Duo diffractometer (Madison, WI, USA) with  $\text{MoK}\alpha$  X-rays ( $\lambda = 0.71073 \text{ \AA}$ ). Crystal specimens were isolated from their mother liquor and immediately placed under Paratone N oil (Exxon, Chemical Co., TX, USA) to minimise spontaneous water loss. They were mounted on nylon cryoloops for data-collection at 100 K in a stream of nitrogen from a cryostream cooler (Oxford Cryosystems Ltd., Oxford, UK). Structure solution and full-matrix least-squares refinement were performed using programs in the SHELX suite.<sup>22</sup> For both complexes, direct methods revealed the majority of their respective non-hydrogen atoms, which were refined initially

isotropically and subsequently anisotropically. However, for several atoms (ordered and disordered) in each complex, isotropic refinement was retained due to unsatisfactory  $U_{ij}$  values. The structural models were gradually developed by the stepwise addition of atoms located in successive difference Fourier syntheses. For both complexes, structure refinement was somewhat complicated by molecular disorder. Further pertinent details of the structure solutions and refinements appear in section 3.

### 2.6 Solubility studies

The solubilities of the DMB-PRO and DMB-BES complexes were measured in fasted state simulated intestinal fluid (FaSSIF) using a gravimetric procedure. In each case, small accurately weighed samples of pure hydrated complex crystals were added to a vial containing 1.0 ml of the FaSSIF solution buffered at pH 6.5 and stirred continuously at 27  $^{\circ}\text{C}$  during the complex additions, until saturation was achieved. The total mass of each complex added to the solution to reach saturation was estimated by taking the average of the cumulative mass recorded after the penultimate sample addition which resulted in dissolution, and that recorded after the final addition which led to precipitation. The solubility enhancement factors for each of PRO and BES were finally calculated taking into account their proportions by mass in the respective hydrated complex formulae. An Agilent 1220 Infinity LC system (Waldbronn, Germany) consisting of a binary pump with sample degasser, an autosampler, a temperature-controlled column oven and a UV/Vis variable wavelength detector, was used for HPLC analysis. Separation was performed with an Agilent Poroshell 120 EC – C18 threaded column (4.6 mm  $\times$  50 mm  $\times$  2.7  $\mu\text{m}$ ) and the analytical data were recorded and analysed using the Agilent ChemStation program OpenLab CDS ChemStation Edition for LC & LC/MS Systems.<sup>23</sup>

The solutions were filtered with 0.2  $\mu\text{m}$  nylon microfilters, and analysed by high-performance liquid chromatography (HPLC) with an isocratic elution of 60:40 (v/v) acetonitrile: 0.1% TFA water mixture. The flow rate, injection volume and column temperature were 0.6  $\text{mL min}^{-1}$ , 5  $\mu\text{L}$ , 25  $^{\circ}\text{C}$  respectively. Detection wavelengths of 240 and 280 nm were used for progesterone and  $\beta$ -estradiol respectively.

## 3. Results and discussion

### 3.1 $^1\text{H}$ NMR analysis of the complexes

Based on the relative proton integrations for host and guest molecules, both inclusion complexes DMB-PRO and DMB-BES were found to have 1:1 DMB:guest stoichiometric ratios. The proton labelling is shown in Fig. S1 (SI) and the  $^1\text{H}$  NMR spectrum of DMB-PRO and its stoichiometric analysis are shown in Fig. S2 and Table S1 respectively. The  $^1\text{H}$  NMR spectrum of DMB-BES and its stoichiometric analysis are shown in Fig. S3 and Table S2 respectively.



### 3.2 HSM analysis of the complexes

The DMB-PRO complex crystals appeared as clear, regular plates while those of DMB-BES were fractured and irregular (Fig. S4, SI). The events occurring on heating clear DMB-PRO crystals include onset of opacity due to initial dehydration, increasing opacity possibly attributable to phase transitions, and finally complex decomposition, details of which are illustrated in 7 successive micrographs (Fig. S5, SI). Heating the complex DMB-BES led to further crystal fracture, opacity onset, crystal fragmentation, vigorous bubbling due to dehydration, sublimation and decomposition (Fig. S6, SI). The above events could be reconciled with the quantitative TGA and DSC data.

### 3.3 TGA analyses of the complexes

Fig. 1 shows representative combined TGA and dTGA (first derivative) curves for the complexes. DMB-PRO (Fig. 1(a)) displays a mass loss of  $1.2 \pm 0.3\%$  ( $n = 3$ ) due to dehydration occurring in the range  $20.0 \pm 3.4$  to  $62.0 \pm 2.4$  °C. This corresponds to  $1.1 \pm 0.2$  water molecules per complex unit. The anhydrous complex subsequently undergoes decomposition (onset at  $177.3 \pm 6.5$  °C). Dehydration of DMB-BES (Fig. 1(b)) occurred between  $20.1 \pm 1.3$  °C and  $50.4 \pm 0.1$  °C, with a mass loss of  $3.1 \pm 0.1\%$  ( $n = 2$ ), amounting to  $2.9 \pm 0.1$  water molecules per DMB molecule. However, this value was later found to be significantly underestimated due to spontaneous dehydration during sample preparation, and as discussed in section 3.5.2, an accurate estimate of water content was subsequently obtained by an alternative procedure. In contrast to the behaviour of DMB-PRO, following dehydration, DMB-BES underwent a mass loss of  $16.9 \pm 0.5\%$  between  $180.5 \pm 4.6$  °C and  $350.0 \pm 1.3$  °C, indicating the release of one molecule of BES per DMB molecule (calculated value from the final complex formula = 16.4%). This result is in accord with the 1:1 host-

guest stoichiometric ratio obtained by  $^1\text{H}$  NMR analysis. Rapid decomposition of the remaining DMB followed from 350 °C.

### 3.4 DSC analyses of the complexes

Given the significantly different TGA profiles for DMB-PRO and DMB-BES, their DSC curves were likewise expected to display different features (Fig. S7, SI). For both complexes endothermic peaks corresponding to their dehydration steps were evident. However, the loss of the guest from DMB-BES was accompanied by a second major endotherm. Smaller thermal events were also evident in the DSC curves of the complexes and were attributed to both exothermic and endothermic phase transitions.

### 3.5 Structural analyses by single-crystal X-ray diffraction (SCXRD)

**3.5.1 The X-ray structure of DMB-PRO.** The solution and refinement of the crystal structure of DMB-PRO proceeded successfully, with final  $R_1$  and  $wR_2$  parameters of 0.0621 and 0.1555 respectively for 11 155 reflections with  $I > 2\sigma(I)$ . Table S3 (SI) lists crystal data, data-collection parameters and refinement details. With  $Z = 2$  complex units per unit cell in the monoclinic space group  $P2_1$ , the asymmetric unit (ASU) comprises a single 1:1 host-guest inclusion complex and the equivalent of one water molecule comprising two disordered components modelled with partial oxygen atoms only, as the H atoms were not evident in the difference Fourier maps. The mode of guest inclusion is shown in stereoscopic view in Fig. 2, which indicates that the progesterone molecule is inserted within the DMB cavity from the wider secondary side of the host molecule, with the acetyl group on the D-ring of the PRO molecule lodged uppermost, abutting the narrower primary side of the host molecule. Also evident in Fig. 2 is an important, well-established feature of the host molecule, namely the formation of a set of seven homodromic O-H...O hydrogen bonds (dotted lines) linking contiguous glucose units, and hence maintaining the 'round' shape of the macrocycle.<sup>24</sup>

Fig. 3 shows the atomic numbering of the guest molecule. Inspection of the ring conformations indicated in Fig. 2

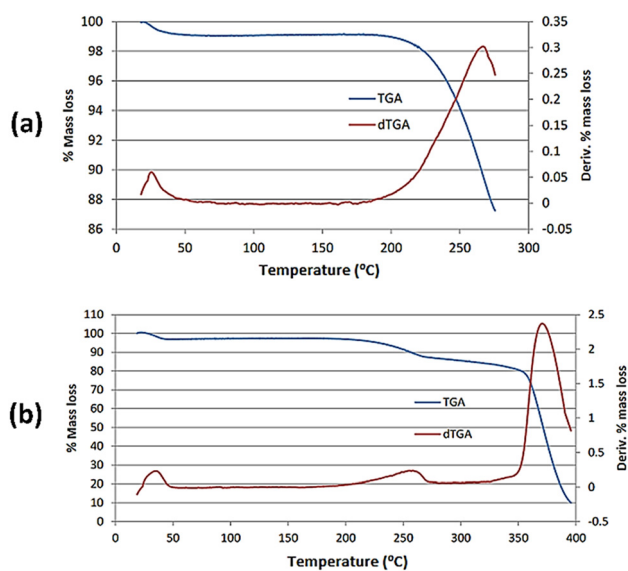


Fig. 1 Representative TGA and dTGA curves for DMB-PRO (a) and DMB-BES (b).

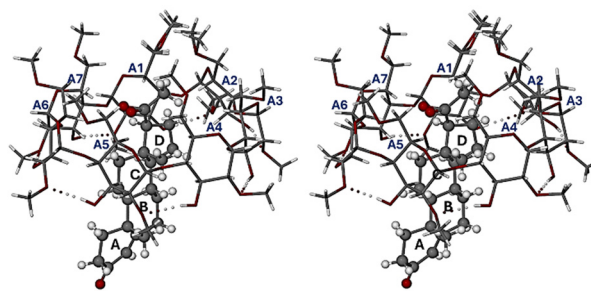


Fig. 2 A stereoscopic view of the complex DMB-PRO which includes the designations A–D of the rings of the steroid molecule, labels A1–A7 assigned to the seven glucose residues in the host DMB molecule, and intramolecular hydrogen bonding in the host molecule (the partial oxygen atoms of the water molecule are omitted for clarity).



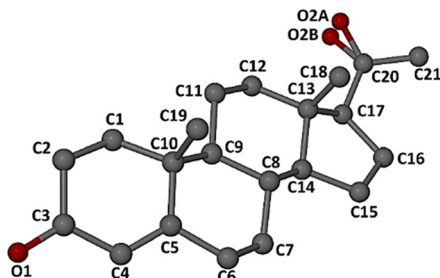


Fig. 3 Numbering of the non-hydrogen atoms in the progesterone molecule. Carbonyl oxygen atom O2 is represented by two disorder components, O2A and O2B, as described below.

revealed that the A-ring adopts a half-chair conformation (C4–C5 being a double bond), while the B- and C-rings are chair-forms, and the D-ring adopts an envelope conformation (flap on C13).

Fig. 2 includes two structural features that require explanation, namely disorder involving two host methoxymethyl groups (on the primary rims of the glucose residues A1 and A2) and disorder of the carbonyl oxygen atom on the acetyl group attached to the steroid D-ring. Detection of these features during least-squares refinement required their modelling, details of which follow. The twofold disorder of the two methoxymethyl groups was accordingly modelled with appropriate bond length restraints, namely 1.43 Å for C–O and 1.51 Å for C–C bonds, with  $\sigma = 0.01$  Å in each case, and isotropic refinement was duly applied to the atoms involved. The carbonyl oxygen atom O2 on the acetyl group of the PRO molecule displayed abnormally high thermal vibration, requiring its treatment as a disordered atom over two ‘split’ positions with restraints on the C=O lengths (1.20 Å,  $\sigma = 0.01$  Å) and the components O2A and O2B were assigned a common isotropic thermal parameter, resulting in their site-occupancy factors (s.o.f.s) refining to the respective values 0.48(1) and 0.52(1).

Two partial oxygen atoms of water molecules, O1W and O2W, within hydrogen-bonding distance of one another (2.79(1) Å) were located, their respective  $U_{\text{iso}}$  values refining to 0.070(4) and 0.057(4) Å<sup>2</sup>, and their s.o.f.s refining to 0.63(2) and 0.53(2). The sum of these s.o.f.s is consistent with the TGA estimate of  $1.1 \pm 0.2$  water molecules per complex unit. The hydrogen atoms of these partial water oxygen atoms did not appear in the difference Fourier map, but the role of the partial water molecules in forming a hydrogen bonded bridge linking two symmetry-related complex units is readily inferred from the relevant O...O interatomic distances.

In Fig. 4, the host and guest molecules are depicted in space-filling representation with different colour schemes (CPK for DMB, while the guest atoms are coloured blue (C), yellow (H) and magenta (O)). Fig. 4a is a side view of the complex unit from which it is evident that rings C and D of the PRO molecule are fully encapsulated within the host cavity, while rings A and B protrude from the (wider) secondary rim of the DMB molecule. This is more evident in Fig. 4b, a cutaway view, which

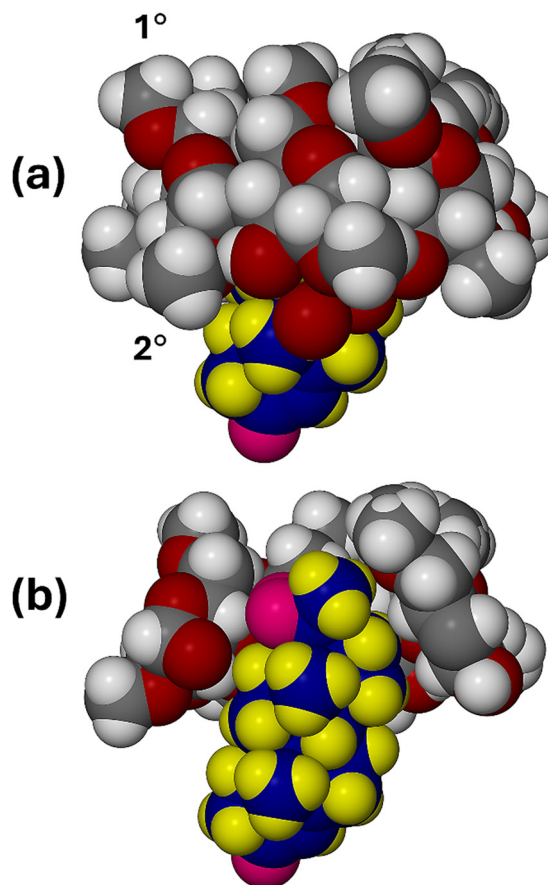


Fig. 4 The complex unit drawn in space-filling mode (a) and a cutaway view (b). The symbols 1° and 2° refer to the primary (narrower) rim and the secondary (wider) rim of the host molecule respectively.

also indicates that the extent of penetration of the guest within the DMB cavity is sterically limited, partly due to the presence of two methoxymethyl groups on the host primary rim. Only one relatively weak hydrogen bonding host–guest interaction (DMB)C–H...O2B(PRO) was detected, O2B being one of the included O2 disorder components. The relevant parameters are C5A6–H5A6...O2B, with H...O 2.52 Å, C...O 3.40(1) Å and angle C–H...O 147°.

With a significant portion of the PRO molecule protruding from the secondary side of the DMB molecule, close packing of the complex units is achieved by insertion of the protruding residue of one complex unit into an interstitial site created by four neighbouring coplanar complex units (Fig. S8, SI). Finally, with regard to the conformation of the DMB host molecule complexed with PRO, detailed analysis of numerous geometrical parameters<sup>25</sup> that measure the distortion of the host upon complexation were calculated and these are provided (Table S5, SI). The main conclusion drawn from these data is that the inclusion of the PRO molecule in DMB did not cause a significant change in the host conformation. In particular, the measured range of the tilt angles (defined in the SI) of the seven glucose units (3.7–24.5°) is practically identical to that for uncomplexed DMB (3.6–24.3°).<sup>24</sup> In addition, the observed lack of strong host–



guest interactions mentioned above is consistent with the notion of relatively small conformational adjustments of both the host and guest molecules involved in their 'mutual induced fit' during the complexation process.<sup>26–28</sup>

**3.5.2 The X-ray structure of DMB-BES.** Structure solution and refinement of the DMB complex containing 17 $\beta$ -estradiol (BES) resulted in a model with final  $R_1$  and  $wR_2$  parameters of 0.0680 and 0.1693 respectively for 31 422 reflections with  $I > 2\sigma(I)$ . This complex also crystallized in the monoclinic chiral space group  $P2_1$ , but in contrast to DMB-PRO, whose ASU contains a single 1:1 DMB-PRO complex unit, the ASU of DMB-BES comprises two independent 1:1 complex units as well as a total complement of 11.6 water molecules. As will be evident in the discussion that follows, the most noteworthy feature of the X-ray structure of DMB-BES is that the orientation adopted by the  $\beta$ -estradiol molecule within the cavity of one of the DMB molecules is opposite to that of the  $\beta$ -estradiol molecule in the other DMB molecule, thus presenting a rare example of bimodal guest inclusion within the same crystal.

Structural refinement was complicated by molecular disorder, several carbon and oxygen atoms of the hydroxyl and methoxy groups of both DMB molecules displaying strongly prolate ellipsoids following anisotropic refinement. For these atoms, the required split into their disorder components was adopted and the latter were accordingly refined isotropically. C–O and C–C bond length restraints analogous to those used in the refinement of DMB-PRO were applied where necessary. On the matter of disorder, it should also be mentioned that while DMB molecules are methylated exclusively at the O2- and O6-positions on each glucose ring, minor disorder in the form of partial methylation can occasionally occur at O3, as we have reported earlier.<sup>28</sup> In the present study, partial methylation at O3 was detected on one of the two DMB molecules in the ASU, namely molecule B. This disorder was modelled as a combination of a partial hydrogen atom (for the partial –OH group) and a partial methyl group, least-squares refinement yielding s.o.f.s of 0.66(3) for the major component, atom H3B5, and 0.34(3) for the partial methyl group. This accounts for the chemical formula of the ASU containing the DMB molecule A ( $C_{56}H_{98}O_{35}$ ) and the partially methylated DMB molecule B ( $C_{56.4}H_{98.8}O_{35}$ ) (Table S4 (SI)). A reliable determination of the water content in the fully hydrated DMB-BES crystal used for SCXRD was obtained by direct location of ordered and disordered water oxygen atoms in the difference Fourier map, their refinement and quantification, as well as confirmation *via* the SQUEEZE procedure implemented in program PLATON.<sup>29</sup> In summary, the total water content was estimated at 11.6 H<sub>2</sub>O molecules per ASU, located over 15 sites. Subsequent deletion of the water oxygen atoms from the SCXRD model and application of the SQUEEZE routine yielded an electron count of 111 per ASU, in reasonable agreement with the theoretical value of 116 electrons for 11.6 water molecules.

Table S4 (SI) lists crystal data, data-collection parameters and refinement details for the DMB-BES complex. Fig. 5 is a stereoscopic view of the two independent complex units A

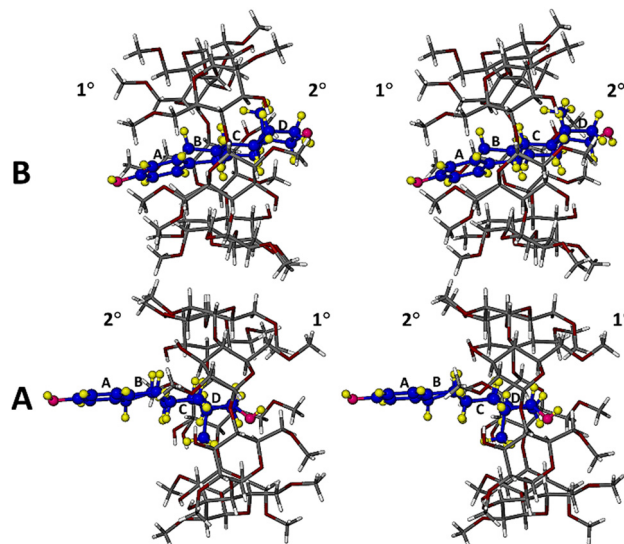


Fig. 5 Stereoview of the structurally distinct DMB-BES complex units A and B in which the orientations of the included  $\beta$ -estradiol guest molecules are reversed.

and B, as they occur in the crystal of DMB-BES. It is evident that in complex unit A, the D-ring of the included  $\beta$ -estradiol molecule is located near the narrow, primary side (designated 1°) of its host molecule, whereas in complex unit B, the D-ring of the included  $\beta$ -estradiol molecule is located at the wide, secondary (2°) rim of its host molecule. This is the major feature of the bimodal inclusion referred to earlier. In addition, it is evident that in complex unit B, the guest molecule appears to be nearly fully encapsulated within the host cavity, while in complex unit A, a significant portion of the  $\beta$ -estradiol molecule protrudes from the host cavity. This protrusion results from bifurcated hydrogen bonding between the hydroxyl group on the D-ring of the BES molecule in complex A and water oxygen atoms located near the primary side of host molecule A (further details of this hydrogen bonding arrangement appear in a later figure).

Fig. 6 is a modified stereoview of Fig. 5, with atoms drawn in space-filling mode to emphasise the extents of guest molecule protrusion in complex unit A and encapsulation in complex unit B.

The atomic numbering and conformations of the two independent guest molecules (A and B) of  $\beta$ -estradiol are shown in Fig. 7. Inspection of the ring conformations of the two independent steroid molecules reveals that for both, ring A is aromatic and hence planar, ring B is a half-chair, ring C is a chair and ring D is an envelope (on C13A for molecule A and on C13B for molecule B). However, a least-squares overlay of molecules A and B (Fig. S9, SI) yields a RMSD value of 0.223 Å, with a maximum deviation of 0.498 Å, indicating small, but significant conformational differences which are expected, given the radically different modes of inclusion of the guest molecules in their respective host cavities. Furthermore, together with significant observed differences in the respective conformations of the host molecules



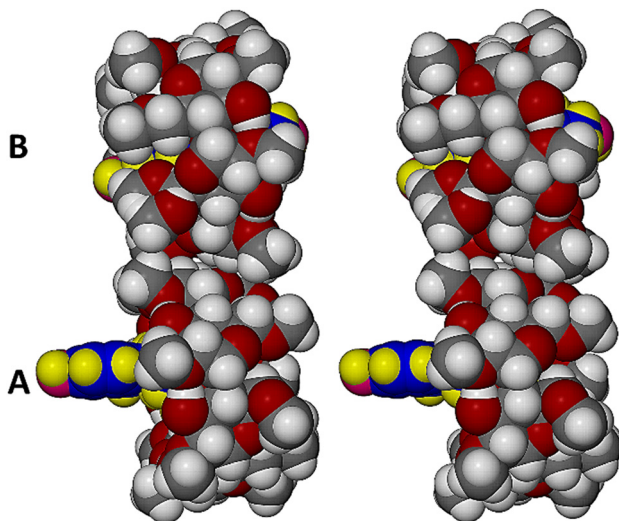


Fig. 6 Stereoview of complex units A and B with atoms in space-filling mode. Guest atoms are coloured yellow (H), blue (carbon) and magenta (O).

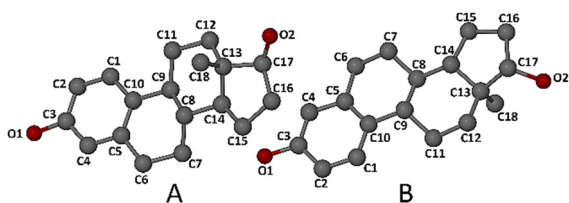


Fig. 7 Numbering of the non-hydrogen atoms in the two independent  $\beta$ -estradiol molecules (A and B), which are drawn in their structural relationship found in the crystal, their respective host molecules being omitted.

(discussed later), the observed differences in the guest conformations are consistent with the mechanism of ‘mutual induced fit’ occurring during complexation,<sup>26–28</sup> a common phenomenon in biological chemistry but one that is seldom observed for relatively small molecular host–guest systems.

Detailed descriptions of the significantly different modes of inclusion of the BES molecules in their respective complex units A and B are warranted. Fig. 8 is a view of complex unit A from the (narrow) primary side of the DMB molecule, from which it is evident that the extent of inclusion of the guest molecule in the DMB cavity is severely limited due to host···water···guest interactions.

The hydroxyl group on the D-ring of the BES molecule engages in bifurcated hydrogen bonds  $O2A-H\cdots O1W$  and  $O2A-H\cdots O6W$ ,  $O1W$  and  $O6W$  being water oxygen atoms that are included in the uppermost part of the host cavity. These oxygen atoms are in turn H-bonded to host methoxy oxygen atoms  $O6A2$  and  $O6A7$  respectively. The two methylated glucose residues A2 and A7 are thus linked by the hydrogen bonded chain with non-H atom sequence  $O6A2\cdots O1W\cdots O2A\cdots O6W\cdots O6A7$ . Thus, there is no direct host–guest interaction, but rather guest inclusion mediated by bridging water molecules. The four  $O\cdots O$  distances in the above chain are respectively 2.808(6), 2.697(6), 2.792(7) and

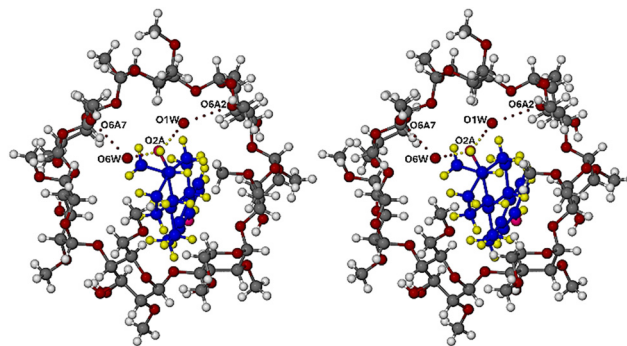


Fig. 8 Stereo-view of complex unit A viewed from the host primary side.

2.907(6) Å, the two shorter distances indicating strong  $O2A\cdots$ water H-bonds. Complexation involving water mediation is not uncommon, another exemplary case being DMB complexation with the antioxidant resveratrol reported earlier.<sup>30</sup>

The (wider) secondary rim of the DMB molecule in complex unit A adopts the well-known ‘round’ shape (Fig. 8), owing to the ‘belt’ of seven intramolecular  $O-H\cdots O$  hydrogen bonds<sup>24</sup> (not shown for clarity, but analogous to that shown for DMB-PRO in Fig. 2). Protrusion of the A ring and part of the B ring of the BES molecule from the secondary rim of the host molecule is thus unhindered. Table S6 (SI) lists the geometrical parameters for the DMB molecule A. The ‘shallow’ mode of inclusion of the BES molecule resulted in a relatively narrow range of the glucose residue tilt angles ( $\tau_2$ ), namely 4.7–16.6°, compared with 3.6–24.3° for uncomplexed DMB,<sup>24</sup> indicating less distortion in host molecule. Fig. 8 also shows that three of the primary methoxymethyl groups are rotated away from the host cavity while the remaining four groups are rotated towards the cavity, acting as a partial ‘lid’, with the oxygen atoms of water molecules  $O1W$  and  $O6W$  adding further obstruction on the primary side.

In Fig. 9, a view of complex unit B from the primary side of the DMB molecule, it is clear that the BES molecule spans the full height of the host molecule, with the hydroxyl group on the steroid A-ring uppermost, at the level of the primary methyl groups, as a result of this BES molecule having the opposite orientation to that of the BES molecule shown in

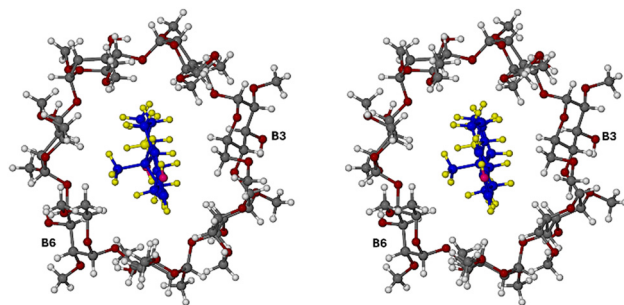


Fig. 9 Stereo-view of complex unit B viewed from the host primary side.



Fig. 8. It is also evident from the asymmetry of the glucose units of host molecule B that full encapsulation of the BES molecule involves considerably more host distortion during complexation than that occurring in host molecule A. This is confirmed from the data in Table S7 (SI) listing the geometrical parameters for DMB molecule B. The range of the glucose tilt angles ( $\tau_2$ ) is 4.6–27.0°, but in this case there are two prominent tilt angle values, namely 24.2° (residue B3) and 27.0° (residue B6). Once again, the phenomenon of mutual induced fit accompanying complexation is evident, reflected in significant changes in the geometrical parameters of the host and guest.

In addition to the tilt angle parameter, the length D3 (the O2...O3' intra-ring distance) is also diagnostic in the present case. The  $D_3$  distance ranges for host molecules A and B are 2.739(5) – 2.865(6) Å and 2.742(6)–3.013(6) Å respectively, the wider range resulting from the more extreme tilt angles in DMB molecule B.

Thus far, attention has been focused on the molecular structures of the complexes DMB-PRO and DMB-BES. In addition to the primary host-guest, host-water and water-water interactions already described, O-H...O and C-H...O hydrogen bonds stabilize their crystal structures. In DMB-PRO, with only one water molecule per complex unit, modelled as two partial water oxygen atoms O1W and O2W within hydrogen bonding distance (2.79(1) Å), it was noted that these atoms are in turn hydrogen bonded to oxygen atoms of the host molecule (O...O distance range 2.79(1)–3.01(1) Å). Crystal cohesion is maintained by several host-host C-H...O hydrogen bonds. However, the DMB-BES complex contains a much larger complement of water molecules, namely 11.6 per ASU, which give rise to several C-H...O(water) hydrogen bonds with C...O distance range 3.128(10)–3.382(11) Å. Several weak host-host C-H...O hydrogen bonds (with C...O > 3.3 Å) contribute to crystal stabilization.

The efficient encapsulation of guest molecules PRO and BES by the host DMB, and hence our ability to obtain detailed structural information for the respective complexes, is in sharp contrast to the results obtained for the corresponding complexes with  $\beta$ -CD and  $\gamma$ -CD,<sup>11</sup> where severe guest disorder prevented their modelling. These different outcomes are primarily due to the radical differences in the nature of the cavities of the parent CDs and that of DMB,<sup>1–4</sup> the latter featuring primary and secondary rims which are both significantly extended by the presence of seven methyl groups that increase the length of the cavity and its apolar nature. This modified cavity topology and its increased hydrophobicity strongly favour the inclusion of elongated lipophilic guest molecules, such as PRO and BES, increasing the extent of hydrophobic and van der Waals host-guest interactions, and thereby stabilising the complex structures. However, for steroidal molecules, this does not guarantee complete guest encapsulation in all cases because of the known flexibility of the methoxymethyl groups on the primary rim of DMB, whose conformations can range from

being fully extended (resulting in an 'open' primary side) or folded (creating a 'lid' on the primary side). Thus, partial encapsulation of the PRO molecule in DMB (Fig. 4) occurs mainly because its D-ring engages in favourable hydrophobic interactions with methoxymethyl groups on the primary rim. On the other hand, full guest encapsulation, involving extended conformations of the methoxymethyl groups, is achieved in complex unit B of DMB-BES (Fig. 9), but partial encapsulation occurs in complex unit A (Fig. 8), where strong hydrogen bonding between the hydroxyl group on the guest D-ring and water molecules dictates the extent of guest inclusion.

### 3.5.3 Further considerations of bimodal guest inclusion.

Returning to the major structural difference between the two complex units in the asymmetric unit of DMB-BES highlighted in preceding figures, namely the occurrence of bimodal guest inclusion, this feature warrants further commentary since the term 'bimodal inclusion' in the context of cyclodextrin complexation has different manifestations. Detection of bimodal inclusion of guest molecules in cyclodextrins in solution has been reported fairly frequently, an earlier case featuring the use of NMR spectroscopic techniques and Job plots to establish the simultaneous occurrence of two distinct 1:1  $\beta$ -CD-(diclofenac sodium) complexes in aqueous solution, involving the inclusion of diclofenac anions in the respective CD cavities with opposite orientations.<sup>31,32</sup> More recently, the same techniques were employed to detect two distinct modes of inclusion of the pentacyclic triterpenoid ursolic acid in amino-appended  $\beta$ -CD molecules in aqueous solution.<sup>33</sup> Rhodamine derivatives containing both a phenyl and a bulky xanthenyl residue have similarly been shown to display bimodal ('phenyl-in', 'xanthenyl-in') inclusion modes in DMB in aqueous solution.<sup>34</sup> In this instance, plausible structures of the resulting complexes were deduced from NMR spectroscopic data. However, from the literature, it appears that the unequivocal detection of bimodal guest inclusion in cyclodextrins in the solid state is not as common. Evidently, the earliest instance of such detection was based on analysis of the phosphorescence decays of  $\beta$ -CD complexes of the guests xanthione and 4*H*-1-benzopyran-4-thione.<sup>35</sup> This methodology was suggested as a possible new approach to studying the existence of different guest orientations within both a solution-state and a solid-state CD complex. However, it should also be recognized that different manifestations of bimodal inclusion in the solid state are possible, *e.g.*, different guest orientations or other modes of their inclusion of a common guest might occur (a) within different individual solid-state inclusion complexes of the common CD host, or (b) within the same crystalline phase. An example in type (a) featured the first isolation of two distinct crystal structures of a 1:1 CD complex, bis( $\beta$ -cyclodextrin)bis(4-hydroxybenzoic acid methyl ester), which was reported in 2003.<sup>36</sup> The monoclinic phase (space group *C*2) and the triclinic phase (space group *P*1) were isolated at different temperatures. Single-crystal X-ray diffraction (SCXRD) revealed that in each of these crystals, two guest molecules are encapsulated within a dimeric  $\beta$ -CD cage, but since the dimer symmetries differ in the



two crystals, the immediate environments of the encapsulated guests differ, thus resulting in distinct, bimodal guest inclusion arrangements. Analogous results were reported recently for two distinct 2:1 hydrated  $\beta$ -CD-fluconazole inclusion complexes, again involving their crystallization in space groups *P1* and *C2*.<sup>37</sup> The low frequency of occurrence of such cases in the literature may be due to lack of experimentation with complex preparation under different conditions, or alternatively, if multiple crystalline forms of a given CD complex are identified by PXRD alone, due to the inability to characterize one or more forms by SCXRD to determine detailed inclusion modes.

The present study, however, features the apparently rare occurrence of bimodal guest inclusion of a CD complex manifested within the same crystal, representing also the first example of this phenomenon involving a steroidal guest molecule, namely the prominent hormone  $\beta$ -estradiol. Interest in the question of the preferred orientation of steroid molecules in CD cavities has been long-standing, and as such, a brief summary of some insights from computational methods of investigation of this phenomenon is warranted. Early predictions of the preferred orientation adopted by steroid molecules in their complexation with CDs in aqueous medium were based on studies using spectroscopic and other techniques. For example, from an early study of 18 steroids with the three native CDs, Uekama *et al.* reported results indicating that the A-ring of the steroid molecule was predominantly included in the cavities of the CDs.<sup>38</sup> However, this topic of preferred orientations has been addressed by more advanced computational techniques in recent years. For example, Cai *et al.* developed a flexible docking algorithm that enabled simulation of the inclusion of twelve steroid molecules in  $\beta$ -CD and  $\gamma$ -CD in aqueous solution with entry of each guest molecule exclusively through the secondary side of each host, and with either the A-ring of the steroid entering first ('A-ring up') or the D-ring entering first ('D-ring up').<sup>14</sup> These tests for bimodal inclusion preferences led to the conclusion that for most of the steroids, the preferred orientation in the CD cavity is A-ring up. However, for three of the steroids with  $\beta$ -CD and four with  $\gamma$ -CD, the D-ring up orientation was favoured and attributed to steric hindrance. In a subsequent study,<sup>17</sup> the possible modes of inclusion of hydrocortisone, progesterone and testosterone in  $\beta$ -CD were studied using molecular dynamics simulations and free-energy computations. An interesting general observation was that, regardless of steroid orientation in the host cavity, partial guest inclusion, rather than complete encapsulation, predominated. Not surprisingly, the study indicated that the primary forces involved in complexation are van der Waals and hydrophobic interactions.

To our knowledge, no analogous computational studies have been performed with dimethylated  $\beta$ -CD (DMB) as host molecule. However, we note that in our SCXRD study, several unique features were observed, the DMB-PRO complex unit featuring partial guest inclusion with guest orientation D-ring up, while the two unique DMB-BES complex units manifest both partial and complete inclusion in the same crystal. Furthermore, complex unit A of DMB-BES features 'D-ring up'

guest orientation, while unit B features 'A-ring up'. In addition, the mode of inclusion of  $\beta$ -estradiol in complex unit A of DMB-BES involves the mediation of water molecules *via* host...water...guest hydrogen bonding, a structural feature that would generally not be evident using computational methods alone.

**3.5.4 API solubility enhancements.** The selection of FaSSIF solution, rather than water, as the medium for solubility measurements was based on the bio-relevance of the former simulated intestinal fluid which contains bile salt and phospholipid to mimic the human gastrointestinal fluid. As such, this medium may have a strong influence on the absorption of poorly water-soluble drugs such as PRO and BES. Thus, the solubility of each API was first measured by adding it in excess to a freshly prepared solution of FaSSIF (buffered at pH 6.5) that was then left to stir for 3 days at 27 °C. Following filtration of the respective solutions, the absorbances from the HPLC analyses were determined (Table S8, SI). The measured solubility values for PRO and BES in FaSSIF solution were respectively  $1.0151 \times 10^{-2}$  mg cm<sup>-3</sup> and  $1.0028 \times 10^{-2}$  mg cm<sup>-3</sup>. Thereafter, the solubility of each of the hydrated crystalline complexes DMB-PRO and DMB-BES was determined in duplicate experiments in FaSSIF solution at 27 °C, using a previously used gravimetric procedure,<sup>39</sup> as described in detail in section 2.6. Details of these measurements and calculations are shown in Table S9 (SI). Significant solubility enhancement values [denoted ( $S_{\text{API( CD)}}$ / $S_{\text{API}}$ ), where  $S_{\text{API( CD)}}$  is the solubility of the API content in the CD complex, and  $S_{\text{API}}$  is that of the untreated API] were recorded for both PRO and BES, the respective ranges of these ratios being 24.6–25.6 and 41.3–42.7 (Table S10, SI).

## 4. Conclusions

As indicated in the Introduction, the knowledge base on the structural features of crystalline CD-steroid inclusion complexes is rather limited. This report on the dimethylated  $\beta$ -CD inclusion complexes containing the potent, but poorly water-soluble, steroid hormones progesterone and 17 $\beta$ -estradiol, is a significant addition to the relatively small number of published crystal structures of CD-steroid complexes. Although our previous study of the inclusion of these steroids in both  $\beta$ -CD and  $\gamma$ -CD yielded the four desired crystalline complexes, whose host-guest stoichiometries and water contents were determined accurately, definitive guest inclusion modes and host-guest interactions could not be discerned due to major disorder of the included API molecules. This limitation prompted the present study which focused on dimethylated  $\beta$ -CD as the host, owing to its radically different molecular structure and superior physicochemical properties, including significantly higher aqueous solubility, which could lead to higher bioavailability of the APIs in complex form.

As reported above, the thermal stabilities of the DMB-PRO and DMB-BES complexes were quite different, the former complex retaining the guest until complex decomposition at ~180 °C, while for the latter, a distinct process, namely loss of



the guest BES, commenced at this temperature. However, the remarkable cases of different modes of steroid inclusion observed in this study have certainly been the focus of this report, rendering these new results informative for researchers engaged in studying both CD–steroid interactions and pharmaceutical complex formulation, and potentially useful to those pursuing computational studies in this area. In summary, for the DMB-PRO complex, partial encapsulation of PRO in the guest cavity was evident, with guest orientation D-ring up. However the DMB-BES complex featured the unusual occurrence of bimodal inclusion manifested in a single crystal, with one of the two crystallographically independent DMB-BES complex units displaying partial guest inclusion and guest orientation D-ring up, while the other features full guest encapsulation, with guest orientation A-ring up. Finally, the ~25-fold solubility enhancement for PRO and the ~42-fold enhancement for BES in the simulated FaSSIF medium represent significant API solubility improvements as a result of their complexation with DMB.

## Author contributions

A. I. V.: investigation; methodology; validation; formal analysis; data curation; visualization. Z. H.: investigation; methodology; validation; formal analysis; data curation; visualization. C. E.-S.: methodology, formal analysis, data curation. M. R. C.: conceptualization; formal analysis; writing article; funding acquisition; project administration; resources; supervision.

## Conflicts of interest

There are no conflicts to declare.

## Data availability

Additional data appear in the supplementary information (SI) file.

Supplementary information: these include <sup>1</sup>H NMR spectra of the two complexes, analyses indicating the host-guest stoichiometries, figures of crystal morphologies and HSM micrographs, representative DSC and TGA curves, tables listing crystal data, data-collection parameters and refinement details, geometrical parameters defining the conformations of the host molecules, calibration curve data for solubility determinations, data for the gravimetric solubility analyses, and tabulated API solubility enhancements. See DOI: <https://doi.org/10.1039/d5ce01106j>.

CCDC 2496606 (DMB-PRO) and 2496610 (DMB-BES) contain the supplementary crystallographic data for this paper.<sup>40a,b</sup>

## Acknowledgements

MRC thanks the University of Cape Town for access to instrumental facilities.

## References

- B. G. Poulson, Q. A. Alsulami, A. Sharfalddin, E. F. El Agammy, F. Mouffouk, A.-H. Emwas, L. Jaremko and M. Jaremko, Cyclodextrins: Structural, Chemical, and Physical Properties, and Applications, *Polysaccharides*, 2022, **3**, 1–31.
- Á. Sarabia-Vallejo, M. del Mar Caja, A. I. Olives, M. A. Martín and J. C. Menéndez, Cyclodextrin Inclusion Complexes for Improved Drug Bioavailability and Activity: Synthetic and Analytical Aspects, *Pharmaceutics*, 2023, **15**, 2345.
- S. Christaki, E. Spanidi, E. Panagiotidou, S. Athanasopoulou, A. Kyriakoudi, I. Mourtzinou and K. Gardikis, Cyclodextrins for the Delivery of Bioactive Compounds from Natural Sources: Medicinal, Food and Cosmetics Applications, *Pharmaceutics*, 2023, **16**, 1274.
- P. Singh and R. Mahar, Cyclodextrin in drug delivery: Exploring scaffolds, properties, and cutting-edge applications, *Int. J. Pharm.*, 2024, **662**, 124485.
- S. K. Araj and Ł. Szeleszczuk, A Review on Cyclodextrins/Estrogens Inclusion Complexes, *Int. J. Mol. Sci.*, 2023, **24**, 8780.
- É. Fenyvesi, I. Puskás and L. Szente, Applications of steroid drugs entrapped in cyclodextrins, *Environ. Chem. Lett.*, 2019, **17**, 375–391.
- D. H. Schwarz, A. Engelke and G. Wenz, Solubilizing steroidal drugs by  $\beta$ -cyclodextrin derivatives, *Int. J. Pharm.*, 2017, **531**, 559–567.
- N. Kanageswaran, M. Nagel, P. Scholz, J. Mohrhardt, G. Gisselmann and H. Hatt, Modulatory Effects of Sex Steroids Progesterone and Estradiol on Odorant Evoked Responses in Olfactory Receptor Neurons, *PLoS One*, 2017, **11**(8), e0159640.
- M. Pilleroová, V. Borbélyová, J. Hodosya, V. Riljakb, E. Renczesa, K. M. Fricke and L. Tóthová, On the role of sex steroids in biological functions by classical and non-classical pathways. An update, *Front. Neuroendocrinol.*, 2021, **62**, 100926.
- L. Kolatorova, J. Vitku, J. Suchopar, M. Hill and A. Parizek, Progesterone: A Steroid with Wide Range of Effects in Physiology as Well as Human Medicine, *Int. J. Mol. Sci.*, 2022, **23**, 7989.
- A. I. Vicatos, Z. Hoossen and M. R. Caira, Inclusion complexes of the steroid hormones 17 $\beta$ -estradiol and progesterone with  $\beta$ - and  $\gamma$ -cyclodextrin hosts: syntheses, X-ray structures, thermal analyses and API solubility enhancements, *Beilstein J. Org. Chem.*, 2022, **18**, 1749–1762.
- A. H. Mazurek, Ł. Szeleszczuk, K. Bethanis, E. Christoforides, M. K. Dudek, M. Zielińska-Pisklak and D. M. Pisklak, 17- $\beta$ -Estradiol- $\beta$ -Cyclodextrin Complex as Solid: Synthesis, Structural and Physicochemical Characterization, *Molecules*, 2023, **28**, 3747.
- P. Saokham, C. Muankaew, P. Jansook and T. Loftsson, Solubility of Cyclodextrins and Drug/Cyclodextrin Complexes, *Molecules*, 2018, **23**, 1161.
- W. Cai, X. Yao, X. Shao and Z. Pan, Bimodal complexations of steroids with cyclodextrins by a flexible docking algorithm, *J. Inclusion Phenom. Macrocyclic Chem.*, 2005, **51**, 41–51.
- C. R. Groom, I. J. Bruno, M. P. Lightfoot and S. C. Ward, The Cambridge Structural Database, *Acta Crystallogr., Sect. B: Struct. Sci., Cryst. Eng. Mater.*, 2016, **72**, 171–179.



- 16 M. Fathallah, F. Fotiadu and C. Jaime, Cyclodextrin Inclusion Complexes. MM2 Calculations Reproducing Bimodal Inclusions, *J. Org. Chem.*, 1994, **59**, 1288–1293.
- 17 W. Cai, T. Sun, P. Liu, C. Chipot and X. Shao, Inclusion Mechanism of Steroid Drugs into  $\beta$ -Cyclodextrins. Insights from Free Energy Calculations, *J. Phys. Chem. B*, 2009, **113**, 7836–7843.
- 18 E. B. Starikov, K. Bräsicke, E. W. Knapp and W. Saenger, Negative solubility coefficient of methylated cyclodextrins in water: A theoretical study, *Chem. Phys. Lett.*, 2001, **336**, 504–510.
- 19 Chemistry Software Solutions, Mestrelab Research, S.L. MestReNova, Version: 6.0.2-5475, (Copyright, 2009).
- 20 Soft Imaging System GmbH, Digital Solutions for Imaging and Microscopy, Version 3.1 for Windows (Copyright, 1987–2000).
- 21 *TRIOS software*, TA Instruments-Waters LLC, 159 Lukens Drive, New Castle, DE19720, USA, 2020.
- 22 G. M. Sheldrick, A short history of SHELX, *Acta Crystallogr., Sect. A: Found. Crystallogr.*, 2008, **64**, 112–122.
- 23 OpenLab CDS ChemStation Edition for LC & LC/MS Systems, Version A.01.05, Agilent Technologies, (Copyright 2001–2013).
- 24 T. Aree, W. Saenger, P. Leibnitz and H. Hoier, Crystal structure of (2,6-di-O-methyl)- $\beta$ -cyclodextrin dihydrate: a water molecule in an apolar cavity, *Carbohydr. Res.*, 1999, **315**, 199–205.
- 25 A. D. French and V. G. Murphy, The effects of changes in ring geometry on computer models of amylose, *Carbohydr. Res.*, 1973, **27**, 391–406.
- 26 T. Sawada, H. Hisada and M. Fujita, Mutual Induced Fit in a Synthetic Host–Guest System, *J. Am. Chem. Soc.*, 2014, **136**, 4449–4451.
- 27 A. Cooper, M. Nutley, E. J. MacLean, K. Cameron, L. Fielding, J. Mestres and R. Palin, Mutual induced fit in cyclodextrin–rocuronium complexes, *Org. Biomol. Chem.*, 2005, **3**, 1863–1871.
- 28 M. R. Caira, S. A. Bourne, H. Samsodien and V. J. Smith, Inclusion complexes of 2-methoxyestradiol with dimethylated and permethylated  $\beta$ -cyclodextrins: models for cyclodextrin–steroid interaction, *Beilstein J. Org. Chem.*, 2015, **11**, 2616–2630.
- 29 A. L. Spek, PLATON SQUEEZE: a tool for the calculation of the disordered solvent contribution to the calculated structure factors, *Acta Crystallogr., Sect. C: Struct. Chem.*, 2015, **71**, 9–18.
- 30 L. Trollope, D. L. Cruickshank, T. Noonan, S. A. Bourne, M. Sorrenti, L. Catenacci and M. R. Caira, Inclusion of trans-resveratrol in methylated cyclodextrins: synthesis and solid-state structures, *Beilstein J. Org. Chem.*, 2014, **10**, 3136–3151.
- 31 A. Mucci, L. Schenetti, M. Vandelli, B. Ruozi and F. Forni, Evidence of the Existence of 2:1 Guest–Host Complexes between Diclofenac and Cyclodextrins in D<sub>2</sub>O Solutions. A <sup>1</sup>H and <sup>13</sup>C NMR Study on Diclofenac/ $\beta$ -Cyclodextrin and Diclofenac/2-Hydroxypropyl- $\beta$ -cyclodextrin Systems, *J. Chem. Res., Synop.*, 1999, 414–415.
- 32 M. Bogdan, M. R. Caira, D. Bogdan, C. Morari and S. Fărcaș, Evidence of a Bimodal Binding between Diclofenac-Na and  $\beta$ -Cyclodextrin in Solution, *J. Inclusion Phenom. Macrocyclic Chem.*, 2004, 225–229.
- 33 S. Song, K. Gao, R. Niu, W. Yi, J. Zhang, C. Gao, B. Yang and X. Liao, Binding behavior, water solubility and in vitro cytotoxicity of inclusion complexes between ursolic acid and amino-appended  $\beta$ -cyclodextrins, *J. Mol. Liq.*, 2019, **296**, 111993.
- 34 Y. Sueishi, Y. Matsumoto, Y. Kimata, Y. Osawa, N. Inazumi and T. Hanaya, Characterization of group-inclusion complexations of rhodamine derivatives with native and 2,6-di-O-methylated  $\beta$ -cyclodextrins, *J. Inclusion Phenom. Macrocyclic Chem.*, 2020, **96**, 365–372.
- 35 M. Sikorski, M. Mira and F. Wilkinson, Photophysics of xanthione and 4H-1-benzopyran-4-thione in  $\beta$ -cyclodextrin Complexes, *Chem. Commun.*, 1997, 395–396.
- 36 M. R. Caira, E. J. C. De Vries and L. R. Nassimbeni, Crystallization of two forms of a Cyclodextrin inclusion complex containing a common organic guest, *Chem. Commun.*, 2003, 2058–2059.
- 37 A. Sala, Z. Hoosen, A. Bacchi and M. R. Caira, Two Crystal Forms of a Hydrated 2:1  $\beta$ -Cyclodextrin Fluconazole Complex: Single Crystal X-ray Structures, Dehydration Profiles, and Conditions for Their Individual Isolation, *Molecules*, 2021, **26**, 4427.
- 38 K. Uekama, T. Fujinaga, F. Hirayama, M. Otagiri and M. Yamasaki, Inclusion complexations of steroid hormones with cyclodextrins in water and in solid phase, *Int. J. Pharm.*, 1982, **10**, 1–15.
- 39 A. I. Vicatos and M. R. Caira, Cyclodextrin complexes of the anticonvulsant agent valproic acid, *CrystEngComm*, 2021, **23**, 6582–6590.
- 40 (a) CCDC 2496606: Experimental Crystal Structure Determination, 2025, DOI: [10.5517/ccdc.csd.cc2psxp3](https://doi.org/10.5517/ccdc.csd.cc2psxp3); (b) CCDC 2496610: Experimental Crystal Structure Determination, 2025, DOI: [10.5517/ccdc.csd.cc2psxt7](https://doi.org/10.5517/ccdc.csd.cc2psxt7).

